Phase–Correlated Imaging from Multi–Threaded Spiral Cone–Beam CT Scans of the Heart

Marc Kachelrieß, Michael Knaup, Willi A. Kalender

Abstract— **Phase–correlated CT, as it is used for cardiac imaging, is the most popular and the most important but also the most demanding special CT application, today. Basically it fulfills the task of depicting a quasi–periodically moving object with significantly reduced motion artifacts. Although the image quality using phase–correlated protocols and reconstruction techniques is significantly better than the image quality obtained with standard (not phase–correlated) techniques there still are motion artifacts remaining and further improvements in temporal resolution are still required. These can be either obtained by further increasing the rotation speed or by having more than one source–detector system rotating around the patient.**

Increasing rotation speed is mainly an engineering issue and due to increased centrifugal forces it appears unlikely to go significantly below the $t_{\mathrm{rot}} = 0.33$ s that are available already. We therefore consider a spiral cone–beam CT scanner that has G tubes and detectors mounted and call this device a multi–threaded or G–threaded CT scanner. Aiming for improved temporal resolution the relative temporal resolution τ is studied as a function of the motion rate (e.g. the heart rate $f_{\mathbf{H}}$) and the degree of scan overlap (i.e. the pitch value p for spiral scans or the number of rotations for a circle scan that corresponds to $1/p$) for various configurations. The parameters to optimize for are the number of threads G and the interthread angles $\triangle\tilde{\alpha}$ and $\triangle\hat{\alpha}$. Due to practical reasons we restrict ourselves to double–threaded ($G = 2$) and triple–threaded ($G = 3$) although our optimization algorithm can cope with any number of threads.

For $G = 2$ we found the optimum whenever the angle between the tubes is $90°$ and when both threads are mounted in the same axial plane. Mounting the threads longitudinally offset results only in a slight reduction of the temporal resolution. The optimum interthread angles for $G = 3$ are $60°$ or $120°$; both result in identical temporal resolution values. We further found that the mean temporal resolution achievable with an optimized multi–threaded CT scanner is a factor of G better than the mean temporal resolution obtained with a single–threaded scanner. This finding meets the expectations.

Approximate image reconstruction of multi–threaded rawdata is performed by modifying the EPBP cone–beam reconstruction algorithm. Reconstructions of a simulated cardiac motion phantom are shown and turn out to improve with increasing G.

I. Introduction

CARDIAC computed tomography challenges the problem of imaging moving objects without showing significant motion artifacts. In general, CT requires at least $180°$ of projection data to perform image reconstruction.[1] This implies that the intrinsic temporal resolution of a standard

---

[1]For fan–beam or cone–beam CT there are some algorithms that can do with a lower scan interval if the object is of adequate shape and if a reduced field of view can be accepted [1]. Here, we will not consider these approaches since they appear too restricted for cardiac imaging.
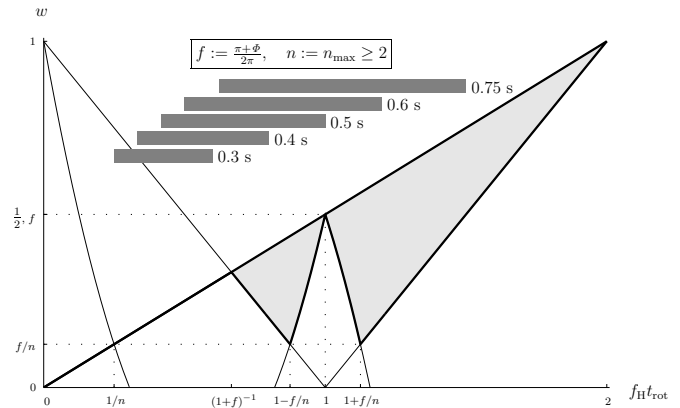
Fig. 1. Temporal resolution vs. heart rate for single–threaded CT (taken with permission from [3]).

CT scan is in the order of $t_{\mathrm{rot}}/2$ or worse, where t_{rot} is the time needed for a full rotation of the scanner. With modern cone–beam CT scanners it is possible to achieve $t_{\mathrm{rot}}/2 = 165$ ms which is not sufficient to perfectly image the anatomical details of the human heart. Standard CT further makes use of all the data contributing to a given voxel and therefore exhibits a temporal resolution of about t_{rot}/p where p is the spiral pitch value (typical values lie in the range $p \in [0.1, 1.5]$).

With dedicated cardiac algorithms it is possible to reduce the data to a single $180°$ segment and achieve $t_{\mathrm{rot}}/2$. If the object is moving in a periodic fashion it is further possible to divide the required $180°$ into several smaller segments and collect these smaller data segments from adjacent motion periods (e.g. heart cylces). Thereby the temporal resolution can be improved proportionally to the number of segments used. One can further align these allowed data intervals (be it one or several segments) to a desired motion phase and obtain images where the object's motion is frozen in the desired state. These basic concepts of phase–correlated CT imaging were first proposed and evaluated in reference [2] and since then they are widely used in clinical CT [3], [4], [5], [6], [7], [8], [9], [10], [11].

Although the use of multi–segment reconstruction combined with very fast rotating scanners appears to provide very high temporal resolution (e.g. 55 ms if three segments are used and a rotation time of 330 ms is assumed) this is rarely the case since the ideal situation where the $180°$ interval can be divided into N intervals of size $180°/N$ only occurs for selected values of $f_{\mathrm{H}} t_{\mathrm{rot}}$ (see figure 1). The average temporal resolution (averaged over the range of typical heart rates) is far from ideal.

Improvements of temporal resolution can also be obtained by equipping a gantry with not only one x–ray tube and one detector but by mounting G tubes and G detectors that rotate together around the patient [12], [13]. If these multiple sources are evenly distributed on a half circle one may expect an improvement in temporal resolution by a factor of G since the 180° of data necessary for image reconstruction can be acquired G times faster than with a single–threaded scanner. To quantify the improvements in view of multi–segment image reconstruction and in view of the complicated behavior of temporal resolution on $f_H t_{rot}$ we have conducted a simulation study. Our study will further seek for the optimal configuration by varying the interthread parameters of the scanner.

Possible applications (including cardiac CT) of G–threaded CT are
- Phase–correlated imaging: This issue is discussed in this paper.
- Motion detection and kymogram processing [14]: The simultaneous acquisition of two or more projections of an object allows to determine the object's position. This can be used to support phase–correlated imaging with the synchronization information.
- Dual energy CT [15]: Using different tube voltages U_g for each thread's tube allows to decompose the rawdata into two base functions (e.g. into the materials water and bone or into the contributions stemming from photo effect or Compton effect).
- Scatter estimation: One thread may be partially used to show scatter information. This may be done by using beamstops. Prior to image reconstruction the missing data can be replaced by another thread's data.
- High–resolution imaging: One thread may have a high resolution detector at the expense of a reduced field of measurement. The high resolution data are truncated but can be easily extended using another thread's data that runs a low–dose acquisition.

II. Geometry

We assume the scanner to have G tubes mounted on one pivot bearing that rotates with constant angular velocity and we assume to have a table that is translated through the rotating gantry with constant velocity parallel to the gantry's rotation axis. The source positions are then given as a function of time t as

$$\boldsymbol{s}_g(t) = \begin{pmatrix} R_g \sin(t + \alpha_g) \\ -R_g \cos(t + \alpha_g) \\ p\,t + z_g \end{pmatrix}$$

with $g = 1, \ldots, G$. To simplify our further considerations we rescaled the temporal axis (t–axis) to obtain a rotation time of $t_{rot} = 2\pi$ and we rescaled the longitudinal axis (z–axis) such that the detector's longitudinal extend is $L = 2\pi$. The table increment per rotation is given as $d = 2\pi p$ from which we see that $p = d/L$ is the spiral pitch value.

R_g is the distance of source g to the isocenter. The possibility of chosing different values of R_g for each thread will

not play a role for us since we assume the temporal information to be associated with the central ray and neglect effects of the finite fan–angle. Thus we may safely assume $R_g = 1$.

III. Data Sufficiency

A z–position z_R is illuminated at

$$t \in T = \bigcup_g T_g \quad \text{with} \quad T_g = \big([-\pi, \pi] + z_R - z_g\big)/p.$$

The projection angles $\alpha = t + \alpha_g$ that are covered during that illumination are

$$\alpha \in A^{\text{Std}} = \bigcup_g A_g^{\text{Std}} \quad \text{with} \quad A_g^{\text{Std}} = T_g + \alpha_g.$$

Standard image reconstruction at z_R can be performed (with an approximate cone–beam algorithm) when A^{Std} covers an angular range of 180° or more.

Here, we are interested in phase–correlated image reconstruction and have a set of synchronization points t_s available, with $t_s < t_{s+1}$. These synchronization points may correspond to the R–peaks of the patient's ECG signal, to the K–peaks of a patient's kymogram or they may correspond to shifted versions of these signals.

Attached to these sync peaks are the allowed data ranges or data segments that are required for reconstruction. The union of all these segments

$$\begin{aligned} S(\tau) &= \bigcup_s \left(t_s + [t_{s-1} - t_s, t_{s+1} - t_s]\frac{\tau}{2} \right) \\ &= \bigcup_s \left(t_s(1 - \frac{\tau}{2}) + [t_{s-1}, t_{s+1}]\frac{\tau}{2} \right) \end{aligned}$$

is the set of time stamps that may enter the reconstruction. The parameter $\tau \in [0, 1]$ is the relative temporal resolution parameter. It is relative since it measures the width of each interval relative to the distance of adjacent sync peaks. Thereby, τ is the fraction of the motion cycle that enters the image. Consequently, the relative temporal resolution τ is a better measure for image quality than an absolute temporal resolution measure where image quality would further depend on the motion rate of the object.

Note that for $\tau = 1$ the intervals touch at the midpoints $\frac{1}{2}(t_s + t_{s+1})$ and we obtain $S(1) = \mathbb{R}$. Thus $\tau = 1$ allows us to mimic a standard image reconstruction situation where all data are allowed to enter reconstruction.

Given a sufficiently large τ the angular contribution of thread g to the desired z–position is $T_g \cap S(\tau) + \alpha_g$ and combining the view angles of all G threads then results in

$$A^{\text{CI}} = \bigcup_g A_g^{\text{CI}} \quad \text{with} \quad A_g^{\text{CI}} = T_g \cap S(\tau) + \alpha_g.$$

Here, CI stands for cardiac interpolation and is used to distinguish from standard image reconstruction. The value of τ must be chosen large enough to ensure A^{CI} to be 180°–complete, i.e.

$$\bigcup_k (A^{\text{CI}} + k\pi) = \mathbb{R}$$

is demanded. Our implementations of cardiac image reconstruction (for single–slice, multi–slice, cone–beam and for G–threaded cardiac CT) use a binary search to determine the minimal possible τ that still ensures $180°$–complete data; an analytic solution to determining τ is not known, to the best of our knowledge.

IV. RELATIVE TEMPORAL RESOLUTION

To determine the actual relative temporal resolution $\hat{\tau}$ that will, in general, differ from the relative temporal resolution parameter τ one must compute the full width at half maximum of the phase sensitivity profile (PSP). The PSP, that was proposed in reference [3], quantifies the contribution of each motion phase to the final image.

Let τ be fixed and large enough such that $A^{\mathrm{CI}}(\tau)$ is $180°$–complete. Thread g contributes the angles $A_g^{\mathrm{CI}} = T_g \cap S(\tau) + \alpha_g$ which is a finite union of disjunct intervals

$$A_g^{\mathrm{CI}}(\tau) = \bigcup_\nu \left(a_{g\nu} + b_{g\nu}[-1,1] \right).$$

We now define multi–triangular weight functions

$$w_g(\alpha) = \sum_\nu \Lambda \left(\frac{\alpha - a_{g\nu}}{b_{g\nu}} \right)$$

where $\Lambda(\cdot)$ is a triangle function of area and height 1. In general, Λ can be replaced by any kind of weight function such as a Gaussian function, for example, as long as $\operatorname{supp} w_g \supseteq A_g^{\mathrm{CI}}$.

We further define the normalization

$$\hat{w}_g(\alpha) = \frac{w_g(\alpha)}{\sum\limits_{k\gamma} w_\gamma(\alpha + k\pi)}$$

which exists since the denominator cannot become zero (remember that A^{CI} is complete).

We achieved

$$\sum_{kg} \hat{w}_g(\alpha + k\pi) = 1 \quad \text{and} \quad \sum_g \int d\alpha\, \hat{w}_g(\alpha) = \pi$$

which implies proper normalization for image reconstruction. This means that each thread must be weighted by its normalized weight function $\hat{w}(\alpha)$ before a slice at z_{R} can be reconstructed. Weighting can also be done in temporal domain using

$$\tilde{w}_g(t) = \hat{w}_g(\alpha - \alpha_g).$$

Now, we use $\tilde{w}_g(t)$ to define the phase sensitivity profile (PSP) that was proposed in [3]. It is defined as the histogram of cardiac phases $c(t)$ weighted by the normalized projection weights $\tilde{w}_g(t)$ as follows:

$$\mathrm{PSP}(c) = \int dt\, \delta(c(t) - c) \sum_g \tilde{w}_g(t)$$

where the cardiac phase $c(t) \in [0,1)$ is defined as

$$c(t) = \frac{t - t_s}{t_{s+1} - t_s}$$

and s is chosen such that $t_s \leq t < t_{s+1}$. The full width at half maximum $\hat{\tau}$ of the PSP is our measure of temporal resolution: $\mathrm{PSP}(0)/2 = \mathrm{PSP}(\hat{\tau}/2)$.
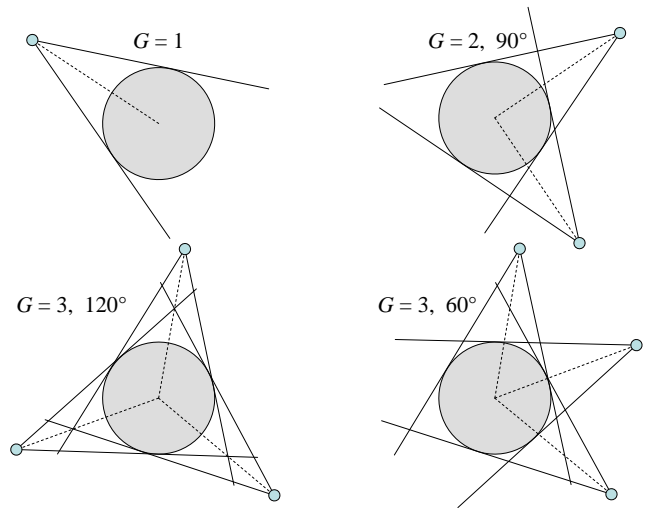
Fig. 2. Winning configurations for $G = 1$, 2 and 3.
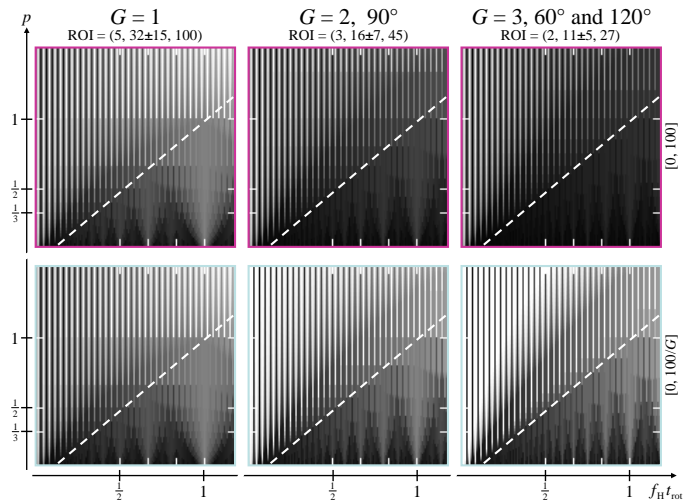
Fig. 3. Plots of temporal resolution $\hat{\tau}$ for single–, double– and triple–threaded scanners as a function of $f_{\mathrm{H}}t_{\mathrm{rot}}$ and p. Images are windowed to the range $[0,1]$ in the upper row and to $[0, 1/G]$ in the lower row. The ROI is defined by $p \leq f_{\mathrm{H}}t_{\mathrm{rot}}$ and is located in the lower right triangle of each plot (indicated by the dashed line). ROI results are given in the form (Min, Mean±StdDev, Max). All temporal resolution values are given in %.

V. SIMULATION STUDY

Our aim is to find a configuration that optimizes temporal resolution over a wide range of heart rates as a function of the multi–threaded scanner geometry. For this we vary G, α_g, z_g and p.

For our simulations we assumed equidistant sync points $t_s = s\Delta t$. Note that $\Delta t/2\pi$ is the ratio of the duration $1/f_{\mathrm{H}}$ of one heart beat to the duration t_{rot} of one gantry rotation. Thereby, we find $f_{\mathrm{H}}t_{\mathrm{rot}} = 2\pi/\Delta t$.

We will further restrict our considerations to the cases $G = 1$, $G = 2$ and $G = 3$ that correspond to a standard, a double–threaded and a triple–treaded spiral cone–beam CT scan, respectively. We also assume equidistant sampling for the interthread angles: $\alpha_g = g\Delta\alpha$ and $z_g = g\Delta z$.
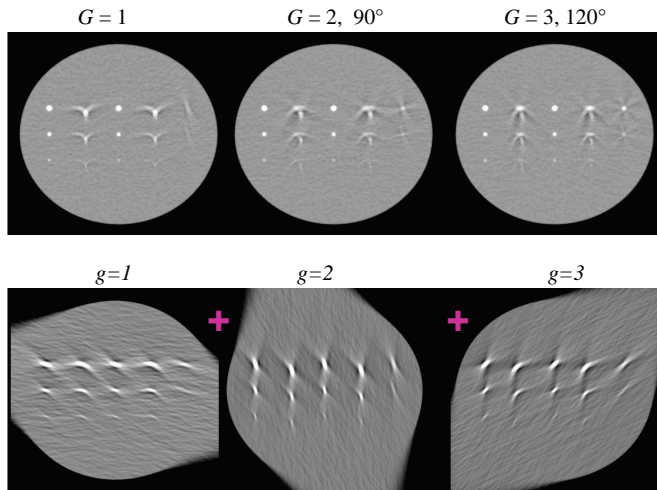
Fig. 4. EPBP reconstructions for up to three threads. The bottom row shows the decomposition of the image for $G = 3$ into the separate threads.

Now, $\hat{\tau} = \hat{\tau}(G, p, \Delta t, \Delta\alpha, \Delta z)$ can be optimized wrt the interthread parameters $\Delta\alpha$ and Δz to cover a wide range of heart ranges Δt and a wide range of pitch values p for some given G.

VI. Results

The optimum scanner configurations that were found by minimizing $\hat{\tau}$ as a function of $\Delta\alpha$ and Δz for a wide range of heart rates and pitch values are shown in figure 2. As expected, $\Delta\alpha = \pi/g$ and $\Delta z = 0$ should be chosen to gain the optimal temporal resolution. Of course symmetry allows to choose $\Delta\alpha = 2\pi/3$ in place of $\pi/3$ for $G = 3$.

Our optimization is based on taking the mean value for the region $p \leq f_H t_{rot}$. Plots that show $\hat{\tau}$ as a function of $f_H t_{rot}$ and p for the three winning configurations are given in figure 3. Here, the ROI $p \leq f_H t_{rot}$ is indicated, too. The figure nicely illustrates the well known resonance phenomena that occur for example when the patient's heart rate is equal to or a fraction of the scanners rotation frequency. In view of the resonance phenomena it is interesting to note that the minimum, the maximum, the mean and the standard deviation of the ROI are approximately proportional to $1/G$. This implies that having a scanner with G threads will have a G–fold performance compared to a single–threaded CT.

To provide image–based evidence the cardiac motion phantom [3] was simulated for $1 \leq G \leq 3$, for a number of configurations (varying interthread parameters) and a number of heart rates. Images were reconstructed with our generalized version of the EPBP algorithm (which is Feldkamp–type, see [10]). An example of a 256–slice spiral scan (1160 projections per rotation, 672 channels per detector row, pitch $1/4$, $t_{rot} = 0.5$ s, slice thickness $S = 0.6$ mm) is shown in figure 4 for a heart rate of 80 min^{-1}. The reconstructions correspond to the fast motion phase of the cardiac motion phantom [3]. One can clearly see highly improved image quality for $G = 3$. This is not so evident for $G = 2$ since figure 4 turned out to show an unlucky situation. In most other cases (not shown) the double–threaded scanner is superior to $G = 1$ but is always inferior to $G = 3$.

VII. Discussion

We analyzed the theoretical performance of a G–threaded spiral cardiac CT to determine the optimal geometry of respective scanners. The results turned out to correspond to the natural choice: $180°/G$ interthread angle and zero longitudinal interthread distance are optimal. Temporal resolution and thus image quality is expected to improve proportional to the number of available threads for all combinations of heart rate, reconstruction phase, rotation time and pitch value. Reconstructions prove that image quality becomes better (less motion and less cone–beam artifacts) with increasing G. Evidently, G–threaded CT seems a promising technique to further enhance CT imaging in general and cardiac CT in particular.

References

[1] F. Noo, R. Clackdoyle, and H. Kudo, "Image reconstruction from fan–beam projections on less than a short scan," *Phys. Med. Biol.*, vol. 47, pp. 2525–2546, 2002.

[2] M. Kachelrieß and W. A. Kalender, "Electrocardiogram–correlated image reconstruction from subsecond spiral computed tomography scans of the heart," *Med. Phys.*, vol. 25, pp. 2417–2431, Dec. 1998.

[3] M. Kachelrieß, S. Ulzheimer, and W. A. Kalender, "ECG–correlated image reconstruction from subsecond multi–slice spiral CT scans of the heart," *Med. Phys.*, vol. 27, pp. 1881–1902, Aug. 2000.

[4] K. Taguchi and H. Anno, "High temporal resolution for multislice helical computed tomography," *Med. Phys.*, vol. 27, pp. 861–872, May 2000.

[5] T. Flohr and B. Ohnesorge, "Heart rate adaptive optimization of spatial and temporal resolution for electrocardiogram–gated multislice spiral CT of the heart," *Journal of Computer Assisted Tomography*, vol. 25, no. 6, pp. 907–923, 2001.

[6] M. Kachelrieß, T. Fuchs, R. Lapp, D.-A. Sennst, S. Schaller, and W. A. Kalender, "Image to volume weighting generalized ASSR for arbitrary pitch 3D and phase–correlated 4D spiral cone–beam CT reconstruction," *Proc. of the 6th Int. Meeting on Fully 3D Image Reconstruction*, pp. 179–182, Nov. 2001.

[7] M. Grass, R. Manzke, T. Nielsen, P. Koken, R. Proksa, M. Natanzon, and G. Shechter, "Helical cardiac cone–beam reconstruction using retrospective ECG gating," *Phys. Med. Biol.*, vol. 48, pp. 3069–3084, 2003.

[8] T. Flohr, B. Ohnesorge, H. Bruder, K. Stierstorfer, J. Simon, C. Suess, and S. Schaller, "Image reconstruction and performance evaluation for ecg–gated spiral scanning with a 16–slice CT system," *Med. Phys.*, vol. 30, pp. 2650–2662, Oct. 2003.

[9] R. Manzke, M. Grass, T. Nielsen, G. Shechter, and D. Hawkes, "Adaptive temporal resolution optimization in helical cardiac cone beam CT reconstruction," *Med. Phys.*, vol. 30, pp. 3072–3080, Dec. 2003.

[10] M. Kachelrieß, M. Knaup, and W. A. Kalender, "Extended parallel backprojection for standard 3D and phase–correlated 4D axial and spiral cone–beam CT with arbitrary pitch and 100% dose usage," *Med. Phys.*, vol. 31, pp. 1623–1641, June 2004.

[11] W. A. Kalender, *Computed Tomography*. Wiley & Sons, 2005. ISBN 3–89578–216–5, 2nd Edition.

[12] R. A. Robb, E. A. Hoffman, L. J. Sinak, L. D. Harris, and E. L. Ritman, "High–speed three–dimensional x–ray computed tomography: The dynamic spatial reconstructor," *IEEE Proc.*, vol. 71, pp. 308–319, Mar. 1983.

[13] Y. Liu, H. Liu, Y. Wang, and G. Wang, "Half–scan cone–beam CT fluoroscopy with multiple x–ray sources," *Med. Phys.*, vol. 28, pp. 1466–1471, July 2001.

[14] M. Kachelrieß, D.-A. Sennst, W. Maxlmoser, and W. A. Kalender, "Kymogram detection and kymogram–correlated image reconstruction from subsecond spiral computed tomography scans of the heart," *Med. Phys.*, vol. 29, pp. 1489–1503, July 2002.

[15] R. Alvarez and A. Macovski, "Energy–selective reconstructions in x–ray CT," *Phys. Med. Biol.*, vol. 21, no. 5, pp. 733–744, 1976.